Reaction of Propargyl with Oxygen

Feng Dong,† Sufan Wang, and Fanao Kong*
Institute of Chemistry, Chinese Academy of Sciences, Beijing 100080, P. R. China
Received: October 14, 2002; In Final Form: August 27, 2003

The elementary reaction of the propargyl radical with the oxygen molecule was experimentally and theoretically investigated. The C_3H_3 radical was produced by laser photolysis of C_3H_3Br at 248 nm. Nascent vibrationally excited products HCO, CO_2, and CO were recorded by time-resolved Fourier transform infrared spectroscopy. The reaction channels of H_2C_2O + HCO (1), CH_3CO + CO (2), and C_2H_3 + CO_2 (4) were identified. For the nascent product CO molecules, a vibrational temperature of 4300 ± 200 K was measured. For the CO_2 product, an inverse vibrational population at $v = 2$ was found. The reaction mechanisms were theoretically investigated by ab initio calculations at the UB3LYP/6-31++G(d,p) level. The calculated results are in agreement with the experimental observations. The highest energy barriers in both channels 1 and 2 are 11.5 kcal/mol, so that the two channels occur at moderate temperature. The energy barrier in channel 4 is 49.3 kcal/mol, restricting the formation of CO_2 to high temperature. These predictions were verified by the quenching effect of argon gas.

1. Introduction

Unsaturated alkyne radicals play key roles in the formation of aromatic compounds, polycyclic aromatic hydrocarbons (PAHs), and soot in combustion process.[1−4] Several experimental and theoretical studies have been carried out on the reaction of ethynyl (C_2H) radical with O_2.[5−8] The measured constants are between 5×10^{-10} and 4.2×10^{-11} cm^3 molecule^{-1} s^{-1}. The products CO and CO_2 have been observed.[8] Propargyl radical is considered a resonantly stabilized free radical. Because of its stability, it can accumulate in relatively high concentrations in flames.[9] The recombination of two propargyl radicals is a major source of compounds with a single aromatic ring such as benzene or phenyl.[10−12] The reaction of propargyl radical with oxygen is the most important competing reaction with the "ring-forming" process. In contrast with C_2H radical, few studies have been performed on the reaction of propargyl (C_3H_3) radical with O_2.

Hudgens and co-workers [13] measured the decay rate of C_3H_3 radical, obtaining the high-pressure limiting rate coefficient k_∞ as 2.3 (± 0.5) × 10^{-13} cm^{-3} molecule^{-1} s^{-1} for the reaction of propargyl with oxygen using cavity ring-down spectroscopy. Slagle and Gutman[14] measured the overall rate constant as 5×10^{-14} exp(−12 kJ mol^{-1}/*RT*) cm^{-3} molecule^{-1} s^{-1} with a tubular reactor coupled with a photoionization mass spectrometer. H_2C_2O was the only product observed. Because many collisions had taken place prior to detection, the species H_2C_2O might not be a nascent product.

Recently, Hahn et al.[15] performed a theoretical analysis of the energetics and pathways of the title reaction at the QCIST (T, full)/6-311++G (3df, 2pd) level. They suggested that the reaction is dominated by the two pathways $C_3H_3 + O_2 \rightarrow CH_2$-CO + HCO and $C_3H_3 + O_2 \rightarrow$ HCCO + H_2CO at high temperatures. Some energetically accessible product channels, such as C_2H_3 + CO_2 (117 kcal/mol) and CH_3CO + CO (109 kcal/mol) were not studied in detail, although similar reaction pathways have been found in the $C_2H + O_2$ reaction.[8]

In this paper, we report experimental and theoretical studies of the reaction $C_3H_3 + O_2$. The nascent excited products HCO, CO, and CO_2 have been observed for the first time by time-resolved Fourier transform infrared (TR-FTIR) emission spectroscopy. New product channels of the reaction were found. Spectral simulations provide relative excited vibrational populations of the products CO and CO_2. The entire reaction mechanism was also investigated by theoretical calculations at the B3LYP/6-31+G(d,p) levels. The results explain the experimental observations very well.

2. Experimental and Theoretical Methods

The experimental apparatus and techniques have been described in detail elsewhere.[16] Briefly, the apparatus consists of a KrF Laser (150 mJ, Lambda Physik-305i), a reaction chamber, and a TR-FTIR spectroscope (Nicolet 800). The infrared emission is collected by a pair of gold-coated spherical mirrors and is recorded by an InSb (77 K) detector, which is sensitive in the region 1800−3600 cm^{-1}. The detector response was taken into account in the simulations. The transient IR emissions of the reaction products were detected 5 μs after laser triggering. The time resolution of the transient recorder is 5 μs, and the spectral resolution is set at 16 cm^{-1}.

A gas mixture of C_3H_3Br (0.3 Torr) and O_2 (0.2 Torr) flows through the reaction chamber. The C_3H_3 radicals are produced by pulsed-laser photolysis of C_3H_3Br at 248 nm.[17] O_2 (≥99.9%, Beijing AP Beifen Gases Industry Company, Ltd.) and C_3H_3Br (80% in toluene, Sigma) were used without further purification. The cross section of C_3H_3Br at 248 nm is about 1×10^{-18} cm^2 molecule^{-1},[18] whereas the cross section of toluene is more than an order of magnitude smaller (about 8×10^{-20} cm^2 molecule^{-1}).[19] The photolysis of toluene thus does not interfere with the study of the $C_3H_3 + O_2$ reaction. We have not observed any IR emission in laser photolysis of a mixture of toluene and O_2.

The detailed reaction mechanism was theoretically investigated with the Gaussian 98 program package.[20] The geometric structures and vibrational frequencies for all stationary points were obtained via density functional theory (DFT) B3LYP using the 6-311++G(d,p) basis set. Intrinsic reaction coordinate (IRC)[21] calculations were further performed to confirm that the transition states connect the right minima at the same level. More reliable energies were determined by single-point DFT//B3LYP/

* Corresponding author. Fax: +86-10-6256-3167. E-mail: kong@mrdlab.icas.ac.cn.
† Graduate student, Graduate Division, Chinese Academy of Sciences.

10.1021/jp027202x CCC: $25.00
Published on Web 10/14/2003

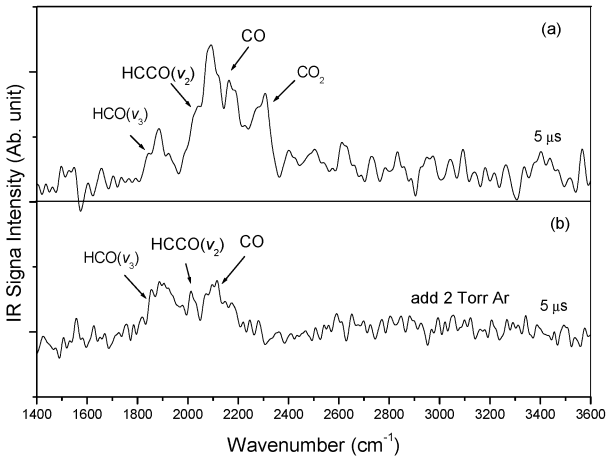

Figure 1. Time-resolved IR emission spectra for the $C_3H_3 + O_2$ reaction at a 5-μs delay time after a KrF laser pulse: (a) mixture of C_3H_3Br (0.3 Torr) and O_2 (0.2 Torr), (b) addition of 2 Torr Ar into the above mixture. Note that the CO_2 peak disappears in spectrum b.

6-311++g(d,p) calculations[22] with inclusion of the B3LYP zero-point vibrational energies (ZPVEs).

3. Results and Discussions

3.1. Reaction Products and Channels. In a reference experiment, only the C_3H_3Br gas (0.2 Torr) was let into the reaction chamber and was irradiated by the KrF laser. No IR emission was observed in this case. However, when the KrF laser irradiated the gaseous mixture of C_3H_3Br and O_2, many IR emission bands appeared in the spectrum. Figure 1a shows the time-resolved IR emission spectra recorded 5 μs after laser triggering. At the partial pressure of 0.2 Torr O_2, only six collisions between C_3H_3 and O_2 species take place within 5 μs. The observed species are thus considered to be the primary products of the reaction.

An emission between 1800 and 1960 cm^{-1} in the IR spectrum is attributed to the transition of vibrationally excited HCO (v_3, the fundamental vibrational frequency being 1868 cm^{-1}).[23] Another emission between 2230 and 2360 cm^{-1} is assigned to CO_2 (v_3, 2341 cm^{-1}). A strong emission between 2020 and 2200 cm^{-1} is assigned to vibratinally excited CO ($v \rightarrow v - 1$) transitions (2143 cm^{-1}). The wide spectral band indicates that the CO products are highly vibrationaly excited. A small hump appears at 2030 cm^{-1}, possibly the v_2 band of HCCO (fundamental vibrational frequency being 2023 cm^{-1}). This feature can clearly be seen when 2 Torr argon gas is added (Figure 1b). The hump might also due to the contribution of $v = 4$ of CO.

The thermodynamically allowed product channels of the reaction are as follows

$$C_3H_3 + O_2 \rightarrow H_2CCO + HCO \quad \Delta H = -91 \text{ kcal/mol} \quad (1)$$

$$\rightarrow CH_3CO + CO \quad \Delta H = -109 \text{ kcal/mol} \quad (2)$$

$$\rightarrow H_2CO + HCCO \quad \Delta H = -71 \text{ kcal/mol} \quad (3)$$

$$\rightarrow C_2H_3 + CO_2 \quad \Delta H = -117 \text{ kcal/mol} \quad (4)$$

$$\rightarrow \underline{CH_2CHO} + CO \quad \Delta H = -104 \text{ kcal/mol} \quad (5)$$

The products generated from these highly exothermic processes must be in vibrationally excited states, and nascent vibrationally excited products HCO, CO_2, and CO were explicitly observed in our TR-FTIR spectrum. This fact indicates that reaction channels 1, 2, and 4 occur, as one of the products for each channel was identified. Channel 3 might also occur.

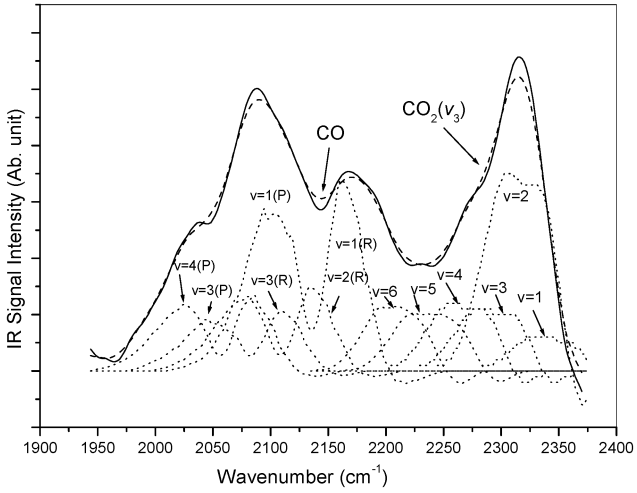

Figure 2. Simulation of the $CO_2 + CO$ spectrum. The spectrum records the emissions of the $C_3H_3 + O_2$ reaction after a 5-μs delay. The dotted curves denote the contributions of the individual $v \rightarrow v - 1$ transitions. The dashed contour is the simulated overall spectrum, and the experimental spectrum is shown by the solid line.

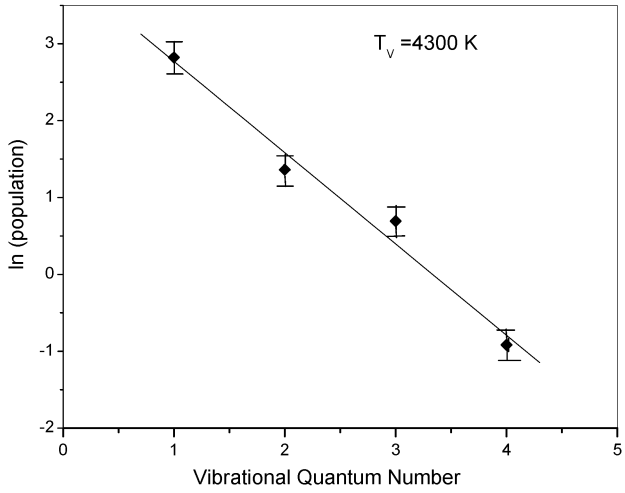

Figure 3. Vibrational distribution of CO (v) 5 μs after the $C_3H_3 + O_2$ reaction. The solid line shows a Boltzmann distribution with a vibrational temperature of $T_v = 4300 \pm 200$ K.

The strong IR radiation emitted from the very "hot" CO should be directly produced in the highly exothermic reaction 2, although some CO might be produced indirectly via further decomposition of HCO or CH_3CO, which are the primary products of channels 1 and 2, respectively. These primary products possess excess energy to overcome their dissociation barriers, 23.5 or 17.8 kcal/mol, for reaction 6 or 7, respectively[24,25]

$$HCO \rightarrow H + CO \quad \Delta H = +16 \text{ kcal/mol} \quad (6)$$

$$CH_3CO \rightarrow CH_3 + CO \quad \Delta H = +11 \text{ kcal/mol} \quad (7)$$

3.2. Spectral Simulations of CO and CO_2. The spectrum of both the CO_2 (v_3) and CO (v) emissions after a 5-μs delay has been simulated. Figure 2 shows the recorded emission spectrum of CO and CO_2 and its simulation. The best-fit rotational temperature was found to be 300 $\pm$ 20 K in the simulation. this result is reasonable if we consider that, within a delay time of 5 μs, the rotational excitation of the nascent

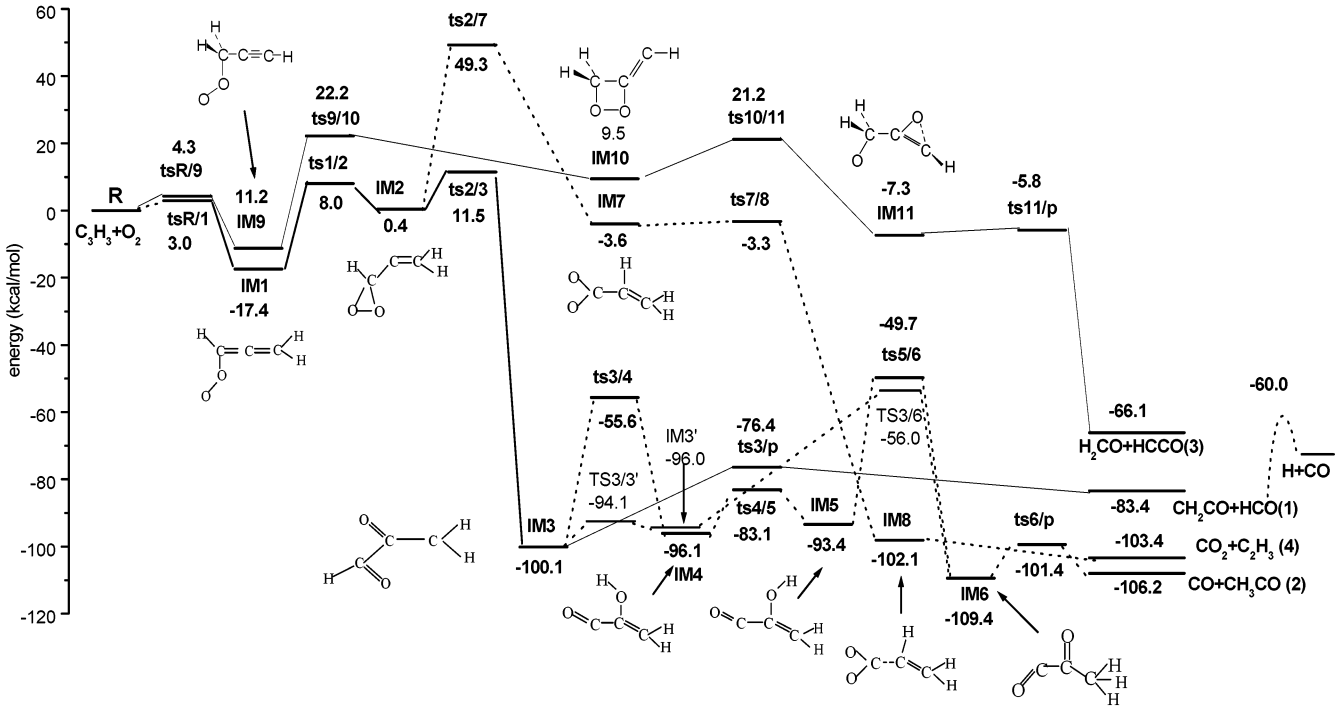

Figure 4. Energy surface of the $C_3H_3 + O_2$ reaction. The energies of the intermediates and transition states in channels 2 and 4 (dotted line) calculated at the UB3LYP/6-31+G(d,p) levels and those in channels 1 and 2 (solid line) are adapted from ref 15.

TABLE 1: Simulated Vibrational Populations of CO (v) and CO_2 (v_3)

v	1	2	3	4	5	6	total
CO	16.8 ± 0.5	3.9 ± 0.3	2.0 ± 0.2	0.4 ± 0.1			23.5
CO_2	0.19 ± 0.05	0.56 ± 0.03	0.12 ± 0.02	0.10 ± 0.01	0.06 ± 0.05	0.04 ± 0.05	1.0

products has almost been quenched. However, vibrational quenching of these small molecules is not expected to be significant during this period. Table 1 lists the simulated vibrational populations of CO and CO_2 (v_3). The population of CO (v) was found to follow a Boltzmanm distribution (Figure 3). The vibrational temperature was estimated as 4300 ± 200 K. It is not likely that all of such CO products yield solely from the dissociation of extremely hot HCO speaks (channel 6). Actually, the moderately excited HCO species still remain in this case. The CO_2 molecule is highly excited in its v_3 mode, with observable population up to $v = 6$ and an inverse distribution at $v = 2$. Because the populations are normalized by Einstein $A(v,j)$ coefficients, the yields of the products can be compared. The yield of CO is estimated to be 23 times greater than the yield of CO_2.

3.3. Reaction Mechanism. Recently, Hahn et al.[15] performed a theoretical analysis of the reaction $C_3H_3 + O_2$. The stationary points on the potential energy surface were found with B3LYP density functional theory. Approximate QCIST (T, full)/6-311++G (3df, 2pd) energies were obtained at these stationary points. Two possible reaction pathways, namely, $HCO + CH_2CO$ (1) and $HCCO + H_2CO$ (***3***), were proposed and are shown in Figure 4 with solid line connections. The energies of the intermediates (IMs) and the transition states (ts's) in channels 1 and 3 are adapted from ref 15. Hahn et al. calculated the rate constants of channels 1 and 3. They concluded that channel 3 is as low as 1% compared with channel 1. However, they did not study two other feasible pathways producing CO and CO_2 in detail.

To understand the reaction mechanism of channels 2 and 4, which lead to the products CO and CO_2, respectively, we performed a theoretical calculation at the DFT/ B3LYP//6-311+G(d,p) level. The potential energy surface (PES) of the two channels is also shown with dotted line connections in Figure 4. The B3LYP-optimized geometries for the possible intermediates and the transient states are shown in Figure 5. In comparison with QCIST the method,[15] Hahn et al. pointed out that the B3LYP well depths were underestimated by approximately 10 kcal/mol.

Both of the resonant structures acetylenic hybrid ($CH_2-C\equiv CH$) and allenic hybrid ($H_2C=C=CH$) of C_3H_3 radical were taken into consideration. The "resonance energy" is approximately 8−9 kcal/mol.[15] The available energy of 68 kcal/mol in the photolysis of C_3H_3Br at 248 nm is very high. The reaction pathways for channels 1−4 were found to be the following

(1) R → tsR/1 → IM1→ ts1/2 →
IM2 → ts2/3 → IM3 → ts3/p → HCO + H_2CCO

(2) R → tsR/1 → IM1 → ts1/2 →
IM2 → ts2/3 → IM3 → ts3/4 → IM4 → ts4/5 →
IM5 → ts5/6 → IM6 → ts6/p → CO + CH_3CO

(IM3 → TS3/3′ → IM3′→ TS3′/6 → IM6)

(3) R → tsR/9 → IM9 → ts9/10 → IM10 →
ts10/11 → IM11 → ts11/p → H_2CO + HCCO

(4) R → tsR/1 → IM1 → ts1/2 → IM2 → ts2/7 →
IM7 → ts7/8 → IM8 → CO_2 + C_2H_3

The first three steps in channels 1 and 2, from reactant R to intermediate **IM3**, are the same. Having overcome a very low barrier of 3.0 kcal/mol, the oxygen molecule attacks the CH side of $H_2C=C=CH$, forming the adduct **IM1** (−17.4 kcal/

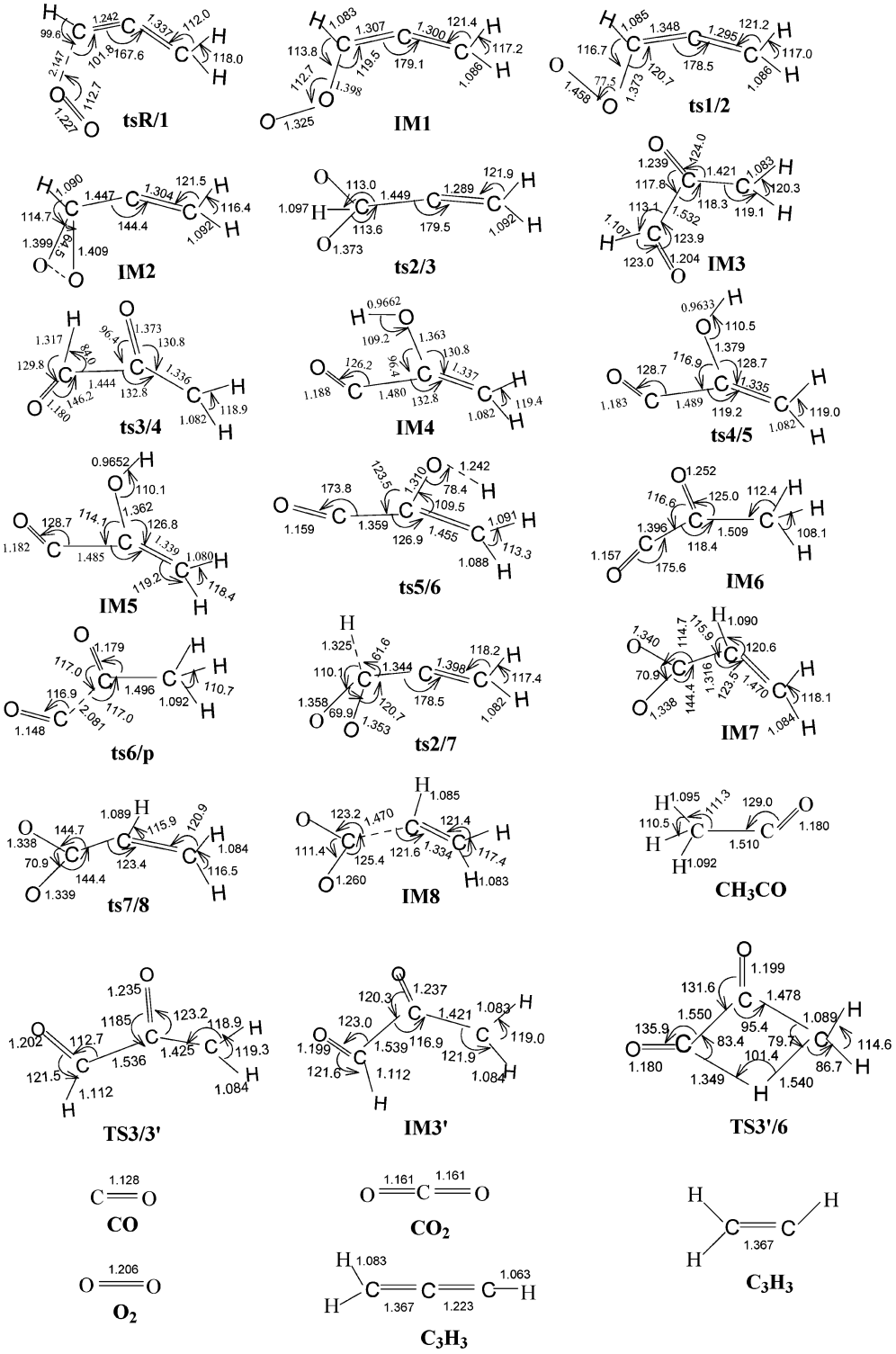

Figure 5. Geometries calculated at the UB3LYP/6-31++G(d,p) level.

mol**)**. Subsequently, a three-membered COO ring forms in the intermediate **IM2** (0.4 kcal/mol) via a transition state **ts1/2**. The O−O bond softens in **IM2**, and then ruptures. The process releases a large amount of energy, yielding the low-energy intermediate **IM3** (−100.1 kcal/mol), CH_2COCHO. In channel 1, **IM3** straightforwardly decomposes to the products HCO + CH_2CO with a barrier of 23.5 kcal/mol. This channel is assumed to be the main pathway of the reaction. The emission of HCO was recorded by the IR spectrometer.

In channel 2, a sequential H-atom migration from the −CHO group of CH_2COCHO (**IM3)** via CH_2CHOCO (**IM4**, **IM5**) to CH_3COCO (**IM6**) takes place. **IM3** can also isomerize to **IM3′** and lead to **IM6** by H-atom migration. The C−C bond of **IM6** breaks, leading to the products CO and CH_3CO. The splitting of channels 1 and 2 occurs in intermediate **IM3**. The barrier heights of **ts3/4** and **ts3/p** are 45.5 and 23.7 kcal/mol, respectively, higher than that of **IM3**, although the entropy changes, $\Delta S^{\ddagger}$, are almost same, being −0.12 and −1.34 cal/(mol K), respectively, referred to **IM3**. According to transition state theory, the product channel branching ratio is determined by both the preexponential factor and the barrier height. The difference between preexponentials is not large, as the $\Delta S^{\ddagger}$

values are comparable. thus, the branching ratio depends mainly on the barrier heights. We conclude that channel 2 is the less favored reaction channel. The overall reaction $C_3H_3 + O_2 \rightarrow CO + CH_3CO$ is exothermic, releasing an energy of 106.2 kcal/mol. The exothermic energy might cause part of the weakly bound CH_3CO radicals to decompose further to CH_3 and CO.

The oxygen molecule can also attack the CH_2 side of $CH_2-C\equiv CH$, yielding the adduct $HCCCH_2OO$ (**IM9**). A ring-closure process in **IM9** forms a four-membered ring intermediate, **IM10**. Cracking of the O−O bond in **IM10** leads to the products H_2-CO and HCCO. Channel 3 is a high-temperature reaction; the product HCCO can be observed in our experiment.

We also found the product of another high-temperature reaction (channel 4), CO_2. Intermediate **IM2** overcomes a high barrier of 49.3 kcal/mol, isomerizing to **IM7**. We believe that this is a concerted reaction involving ring opening and a H-atom shifting. Finally, **IM7** can feasibly dissociate to the final products CO_2 and C_2H_3 via **IM8**. The barrier of **ts2/7** (49.3 kcal/mol) is much higher than that of **ts2/3** (11.5 kcal/mol). Meanwhile, the corresponding entropy changes, $\Delta S^{\ddagger}$, of the two transient states are comparable [−1.7 cal/(mol K) for **ts2/7** and −0.20 cal/(mol K) for **ts2/3** referred to **IM2**]. Thus, reaction channel 4 is the minor one. We could not find any transient states forming $CH_2CHO + CO$.

3.4. Reactions in Ar Gas. The contribution of the various reaction channels depends strongly on their activation energies and the available energy. The barriers in reaction channels 1 and 2 are not high. The two channels are thus considered as the major reaction pathways, which occur at moderate temperatures. Furthermore, channel 1 is more favorable than channel 2 according to their barrier heights. A higher energy barrier of 49.3 kcal/mol exists in the reaction path of channel 4, causing this channel to be important only at higher temperature. We performed an experiment to inspect the feasibility of this sequence. In the experiment, the high translational energy of the hot reactant C_3H_3, which had been produced by UV laser photolysis, was cooled by argon gas. The high-temperature reactions could efficiently be choked, whereas the low-temperature reactions still took place.

The energy of the nascent photofragment C_3H_3 that can be used to overcome reaction barriers is estimated as follows. The available energy in the photolysis of C_3H_3Br at 248 nm is about 68 kcal/mol. According to ref 17, the fraction of total energy released as translation is 42% (28.6 kcal/mol), leaving an internal energy of 58% (39.4 kcal/mol). The translational energy of C_3H_3 radical is estimated as 19 kcal/mol with the instantaneous model, but only 8.8 ± 6 kcal/mol can be used for the reaction according to the study of Zare et al.[26] The internal energy of the C_3H_3 radical is about 39.4 kcal/mol if the other fragment, the Br atom, is in its ground state, $^2P_{3/2}$. Therefore, the total available energy for the title reaction is about 48.2 ± 6 kcal/mol. This energy barely reaches the top of the highest barrier of 49.3 kcal/mol in reaction channel 4. Thus, all reaction channels, from 1 to 4, are open in this case.

If argon buffer gas is added to the cell, the kinetic energy of the C_3H_3 will be quenched by the T−T energy transfer between Ar and C_3H_3 radicals. As a result, the reaction product CO_2 of channel 4 should disappear. This prediction is verified in Figure 1b. Comparing the two spectra in Figure 1 a and b, it can be seen that the CO (v) peak is lowered by one-half by the Ar gas, although the yield of HCO almost unchanged. This implies that channel 1 is the most favored pathway of the reaction, whereas channel **2** is a moderate-temperature reaction and channel 4 is a high-temperature reaction. These observations agree with our predictions very well.

4. Concluding Remarks

The elementary reaction of C_3H_3 radical with O_2 was initiated by laser photolysis of C_3H_3Br at 248 nm, and the reaction products were detected by TR-FTIR emission spectroscopy. The vibrationally excited species HCO, CO, and CO_2 were observed for the first time. The product channels of $H_2C_2O + HCO$, $C_2H_3O + CO$, and $C_2H_3 + CO_2$ were identified.

The vibrational populations of CO ($v = 1-4$) were determined. The vibrational temperature was estimated as 4300 ± 200 K. The ν_3 mode of CO_2 is highly excited up to 6, and its vibrational population was inverted at $v = 2$.

The reaction mechanisms were calculated at the B3LYP/6-31+G(d,p) level and compared with the results reported in ref 17. The O_2 molecule attacks C_3H_3 radicals, forming ring-structured adducts in which the O−O bond softens. The favored reaction pathways involving low-energy barriers are the channels 1 and 2, whereas channel (**4**) is a high-temperature reaction. The above preference was verified by the cooling effect of argon gas.

Acknowledgment. The project was supported by NSFC and NKBRSF projects. The authors also appreciate helpful discussions with Dr. Baoshan Wang.

References and Notes

(1) Lander, D. R.; Unfried, K. G.; Stephens, J. W.; Glass, G. P.; Curl, R. F. *J. Phys. Chem.* **1989**, *93*, 4109.
(2) Lander, D. R.; Unfriend, K. G.; Glass, G. P.; Curl, R. F. *J. Phys. Chem.* **1990**, *94*, 7759.
(3) Miller, J. A.; Melius, C. F. *Combust. Flame* **1992**, *91*, 21.
(4) Kern, R. D.; Singh, H. J.; Wu, C. H. *Int. J. Chem. Kinet.* **1988**, *20*, 731.
(5) Pedersen, J. O. P.; Opansky, B. J.; Leone, S. R. *J. Phys. Chem.* **1993**, *97*, 6822.
(6) Opansky, B. J.; Seakins, P. W.; Pedersen, J. O. P.; Leone, S. R. *J. Phys. Chem.* **1993**, *97*, 8583.
(7) Thiesemann, H.; Taatjes, C. A. *Chem. Phys. Lett.* **1997**, *270*, 580.
(8) Su, H.; Yang, J.; Ding, Y.; Feng, W.; Kong, F. *Chem. Phys. Lett.* **2000**, *326*, 73.
(9) Westmoreland, P. R.; Dean, A. M.; Howard, J. B.; Longwell, J. P. *J. Phys. Chem.* **1989**, *93*, 8171.
(10) Alkemade, U.; Homann, K. H. Z. *Phys. Chem.* **1989**, *161*, 19.
(11) D'Anna, A.; Violi, A.; D'Allessio, A. *Combust. Flame* **2000**, *121*, 418.
(12) D'Anna, A.; Violi, A. *Proc. Combust. Inst.* **1998**, *27*, 425.
(13) Atkinson, D. B.; Hudgens, J. W. *J. Phys. Chem. A* **1999**, *103*, 4242.
(14) Slagle, I. R.; Gutman, D. *Proc. Combust. Inst.* **1986**, *21*, 875.
(15) Hahn, D. K.; Klippenstein; S. J.; Miller, J. A. *Faraday Discuss.* **2001**, *119*, 79.
(16) Zhu, Q.; Huang, S.; Wang, X. *Chin. J. Chem. Phys.* **1993**, *6*, 87.
(17) Lee, Y. R.; Lin, S. M. *J. Chem. Phys.* **1998**, *108*, 134.
(18) Fahr, A.; Hassanzadeh, P.; Laszlo, B.; Huie, R. E. *Chem. Phys.* **1997**, *215*, 59.
(19) Talrose, V.; Stern, E. B.; Goncharova, A. A.; Messineva, N. A.; Trusova, N. V.; Efimkina, M. V. UV/Visible Spectra. In *NIST Chemistry WebBook, NIST Standard Reference Database*; Linstrom, P. J., Mallard, W. G., Eds; National Institute of Standards and Technology: Gaithersburg, MD, Jul 2001; Entry 20899.
(20) Frisch, M. J.; Trucks, G. W.; Schlegel, H. B.; Scuseria, G. E.; Robb, M. A.; Cheeseman, J. R.; Zakrzewski, V. G.; Montgomery, J. A., Jr.; Stratmann, R. E.; Burant, J. C.; Dapprich, S.; Millam, J. M.; Daniels, A. D.; Kudin, K. N.; Strain, M. C.; Farkas, O.; Tomasi, J.; Barone, V.; Cossi, M.; Cammi, R.; Mennucci, B.; Pomelli, C.; Adamo, C.; Clifford, S.; Ochterski, J.; Petersson, G. A.; Ayala, P. Y.; Cui, Q.; Morokuma, K.; Malick, D. K.; Rabuck, A. D.; Raghavachari, K.; Foresman, J. B.; Cioslowski, J.; Ortiz, J. V.; Stefanov, B. B.; Liu, G.; Liashenko, A.; Piskorz, P.; Komaromi, I.; Gomperts, R.; Martin, R. L.; Fox, D. J.; Keith, T.; Al-Laham, M. A.; Peng, C. Y.; Nanayakkara, A.; Gonzalez, C.; Challacombe, M.; Gill, P. M. W.; Johnson, B. G.; Chen, W.; Wong, M. W.; Andres, J. L.; Head-Gordon, M.; Replogle, E. S.; Pople, J. A. *Gaussian 98*, revision A.6; Gaussian, Inc.: Pittsburgh, PA, 1998.

(21) Gonzalez, C.; Schlegel, H. B. *J. Phys. Chem.* **1990**, *94*, 5523.
(22) Pople, J. A.; Head-Gordon, M.; Raghavachari, K. J. *J. Chem. Phys.* **1987**, *87*, 5968.
(23) McKellar, A. R. W.; Burkholder, J. B.; Orlando, J. J.; Howard, C. J. *J. Mol. Spectrosc*. **1988**, *130*, 445.
(24) Jensen, H. J. A.; Jorgensen, P. *J. Chem. Phys.* **1984**, *80*, 1204.
(25) North, S.; Blank, D. A.; Lee, Y. T. *Chem. Phys. Lett.* **1994**, *224*, 38.
(26) Wim, J. V. Z.; Zhang, R.; Zare, R. N.; Mckendrick, K. G.; Valentini, J. J. *J. Phys. Chem.* **1991**, *94*, 5860.